Published in final edited form as:
Cell. 2007 April 20; 129(2): 345–357.

Zfx controls the self-renewal of embryonic and hematopoietic stem cells

Jose M. Galan-Caridad[1,*], **Sivan Harel**[1,*], **Teresita L. Arenzana**[1], **Z. Esther Hou**[1], **Fiona K. Doetsch**[2], **Leonid A. Mirny**[3], and **Boris Reizis**[1]

1 *Department of Microbiology, Columbia University Medical Center, New York, NY, 10032, USA*

2 *Department of Pathology, Columbia University Medical Center, New York, NY, 10032, USA*

3 *Harvard-MIT Division of Health Sciences and Technology, Massachusetts Institute of Technology, Cambridge, MA 02139, USA*

Summary

Stem cells (SC) exhibit a unique capacity for self-renewal in an undifferentiated state. It is unclear whether the self-renewal of pluripotent embryonic SC (ESC) and of tissue-specific adult SC such as hematopoietic SC (HSC) is controlled by common mechanisms. The deletion of transcription factor Zfx impaired the self-renewal but not the differentiation capacity of murine ESC; conversely, Zfx overexpression facilitated ESC self-renewal by opposing differentiation. Furthermore, Zfx deletion abolished the maintenance of adult HSC, but did not affect erythromyeloid progenitors or fetal HSC. Zfx-deficient ESC and HSC showed increased apoptosis and SC-specific upregulation of stress-inducible genes. Zfx directly activated common target genes in ESC and HSC, as well as ESC-specific target genes including ESC self-renewal regulators Tbx3 and Tcl1. These studies identify Zfx as a shared transcriptional regulator of ESC and HSC, suggesting a common genetic basis of self-renewal in embryonic and adult SC.

Introduction

The development and function of multicellular organisms are based on the activity of stem cells (SC). During early embryonic development, pluripotent stem cells give rise to all cell types in the body, including the germ line (Boiani and Scholer, 2005). In the adult, tissue homeostasis is maintained by multipotent adult stem cells, which continuously generate cell lineages comprising a given tissue. In adult mammals, SC have been identified in many tissues and organs, including the hematopoietic system, brain, skin, and intestine (Weissman et al., 2001). Whereas the precise differentiation potential varies between different SC types, all SC share the fundamental property of self-renewal, i.e. the maintenance of their number and identity in an undifferentiated state.

Embryonic stem cells (ESC) can be derived from pluripotent cells of the blastocyst inner cell mass and propagated *in vitro* as continuous clonal lines (Chambers and Smith, 2004). These ESC lines are capable of unlimited growth in culture while retaining their undifferentiated state and full developmental potential. Murine ESC are typically cultured on fibroblast feeder cells

Corresponding author: Boris Reizis phone (212) 305 5793 fax (212) 305 1468 e-mail bvr2101@columbia.edu
*these authors contributed equally to the work

with serum and leukemia inhibitory factor (LIF), a cytokine that activates the essential gp130/Stat3 signaling pathway. Combined with LIF, bone morphogenetic proteins (BMP) support unlimited ESC self-renewal in the absence of serum or feeders (Ying et al., 2003). The pluripotency of ESC is regulated by a unique network of ESC-specific transcription factors including Oct4, Nanog, Sox2, and their binding partners (Boyer et al., 2005;Chambers and Smith, 2004;Wang et al., 2006). Indeed, a defined combination of Oct4, Sox2 and other transcription factors is sufficient to derive ESC-like pluripotent cells from mouse fibroblasts (Takahashi and Yamanaka, 2006). In addition, a distinct genetic pathway regulating ESC self-renewal involves transcription factors Tbx3 and Esrrb and a signaling co-factor Tcl1 (Ivanova et al., 2006).

Among adult SC types, one of the best characterized is the blood-producing hematopoietic SC (HSC) of the adult bone marrow (BM) (Kondo et al., 2003). These cells sustain hematopoiesis throughout adult life, and are capable of clonal, long-term hematopoietic reconstitution of irradiated recipients after serial transplantation. HSC are localized in a distinct structural and functional compartment in the BM, the HSC niche, which provides critical signals supporting HSC self-renewal (Calvi et al., 2003;Zhang et al., 2003). Upon differentiation, the *bona fide* long term-repopulating HSC rapidly lose their self-renewal potential, producing a hierarchy of multipotent short-term HSC and/or multilineage progenitors, common lymphoid and myeloid progenitors, and lineage-committed precursors. In the adult mouse BM, all HSC activity is contained in the rare (<0.1%) lineage marker ($\underline{L}in)^{-}$ $\underline{S}ca\text{-}1^{+}$ c-$\underline{K}it^{+}$ (LSK) cell subset, which can be further subdivided to define the homogeneous long-term HSC population. The self-renewal of adult HSC is regulated by several broadly expressed transcription factors including Bmi-1 (Lessard and Sauvageau, 2003;Park et al., 2003), Tel/Etv6 (Hock et al., 2004) and FoxO (Tothova et al., 2007).

Although both ESC and adult SC are capable of unlimited self-renewal, their cellular and molecular features are strikingly different. First, ESC can self-renew in defined culture conditions *in vitro*, whereas the self-renewal of adult SC typically depends on their *in vivo* niche (Li and Xie, 2005). Furthermore, ESC are highly proliferative and exhibit unusual features of cell cycle control, such as the lack of a G1 checkpoint (Burdon et al., 2002). In contrast, a cardinal feature of adult SC is their low proliferation rate (Li and Xie, 2005). Indeed, genetic manipulations that increase HSC proliferation lead to HSC exhaustion and eventual failure (Cheng et al., 2000;Yilmaz et al., 2006;Zhang et al., 2006). In view of these fundamental differences between ESC and various adult SC, a major unresolved question is whether their self-renewal is regulated by common genes and/or pathways (Eckfeldt et al., 2005;Mikkers and Frisen, 2005). Such "stemness" genes have been postulated on the basis of global expression analysis of different SC populations (Ivanova et al., 2002;Ramalho-Santos et al., 2002); however, they remain to be reconciled between different studies and verified in functional assays (Sakaguchi et al., 2006). Furthermore, other studies emphasized the lack of a common gene expression program in ESC and adult SC (D'Amour and Gage, 2003;Fortunel et al., 2003).

Zfx is a zinc finger protein of the Zfy family, whose members are highly conserved in vertebrates. Mammalian Zfx is encoded on the X chromosome and contains an acidic transcriptional activation domain (AD), a nuclear localization sequence (NLS) and a DNA binding domain (DBD) consisting of 13 C_2H_2-type zinc fingers (Schneider-Gadicke et al., 1989). A targeted mutation of murine *Zfx* resulted in partially penetrant neonatal lethality and hypofertility in surviving females (Luoh et al., 1997). However, the possibility that the targeting created a hypomorphic *Zfx* allele could not be ruled out. Recently, two microarray-based expression studies suggested that *Zfx* might be expressed at elevated levels in several SC types (Fortunel et al., 2003;Ramalho-Santos et al., 2002), prompting us to investigate the role of Zfx in SC function.

Here, we use conditional gene targeting to examine the role of murine Zfx in two prototypical SC types, ESC and adult HSC. We report that Zfx is required for the self-renewal of both SC types, whereas it is dispensable for the growth and differentiation of their progeny. These results establish Zfx as a shared transcriptional regulator of embryonic and adult SC, suggesting a common molecular basis of SC self-renewal.

Results

Conditional targeting of murine Zfx

To confirm the elevated expression of *Zfx* in SC, we measured *Zfx* levels in SC by quantitative PCR (qPCR). As shown in Fig. 1A, the expression of *Zfx* was twice as high in HSC and in undifferentiated ESC compared to their respective differentiated progeny. To test the function of Zfx in SC, we generated a conditional *LoxP*-flanked ("floxed") allele of murine *Zfx* by homologous recombination in ESC (Fig 1B and Suppl. Fig. 1). Cre-mediated recombination of the only Zfx^{flox} allele in male Zfx^{flox}/y cells produced Zfx^{null} allele, which did not encode a detectable protein product (Fig. 1C). Embryos with germ line Zfx deletion developed normally until 9.5 d.p.c. and subsequently died due to extraembryonic tissue abnormalities (data not shown). The embryos with Zfx deletion in the embryo proper died neonatally but were grossly normal at 18.5 d.p.c., with Zfx^{null} cells contributing extensively to all tissues (Suppl. Fig. 2). Similarly, a nearly complete deletion of Zfx in the absence of obvious abnormalities was observed in embryos and newborns with early brain- or hematopoietic-specific Zfx deletion (Suppl. Fig. 2). These data suggest that Zfx is dispensable for cell growth and differentiation of most tissues *in vivo*.

Zfx is required for ESC self-renewal

To analyze the growth of Zfx-deficient ESC, we transiently induced Cre recombination in Zfx^{flox} ESC and cultured the resulting mixture of recombined (Zfx^{null}) and un-recombined ESC in the conditions favoring self-renewal (serum/LIF/feeders). As shown in Fig. 2A, Zfx^{null} ESC were rapidly out-competed by Zfx^{flox} cells and disappeared after two passages. In contrast, Zfx^{null} cells persisted when ESC were allowed to differentiate in the absence of LIF/feeders. Moreover, a similar competition assay revealed normal growth of Zfx-deficient primary mouse embryonic fibroblasts (MEF), confirming a specific role of Zfx in undifferentiated ESC.

To further characterize the phenotype of Zfx-deficient ESC, we derived clonal Zfx^{null} ESC lines and then stably re-expressed Zfx in these cells (Fig. 2B). The resulting Zfx^{null} ESC remained undifferentiated, as judged by the expression of ESC marker alkaline phosphatase (Fig. 2C) and key ESC regulators Nanog and Oct4 (Suppl. Fig. 3). Nevertheless, all Zfx^{null} clones (n=10) exhibited abnormal colony morphology, reduced clonogenic capacity, slower growth and spontaneous apoptosis in serum/LIF (Fig. 2C,D,E). The impaired self-renewal of Zfx^{null} ESC was particularly evident in serum-free culture with LIF and BMP4, in which Zfx^{null} clones failed to expand and collapsed after 2–3 passages (Fig. 2F). During the initial growth in serum-free culture, Zfx^{null} cells underwent massive apoptosis as revealed by increased proportion of Annexin V-positive and hypodiploid cells (Fig. 2G and Suppl. Fig. 3). Notably, nearly all (9/10) Zfx^{null} ESC clones reconstituted with Zfx (Zfx^{null}+Zfx) regained normal morphology and vigorous growth (Fig. 2C,D,F,G). These data demonstrate a specific and reversible defect in the growth and survival of undifferentiated Zfx-deficient ESC.

In contrast to their impaired self-renewal, the differentiation capacity of Zfx-deficient ESC was intact. When injected into mice, Zfx^{null} ESC efficiently produced teratomas containing differentiated tissues from the three germinal layers (Fig. 3A). Despite the low efficiency of chimera formation after blastocyst injection, Zfx^{null} ESC contributed to the majority of adult tissues in chimeric mice, including the germ line (Fig. 3B). The lack of contribution to the

thymus and BM is consistent with the essential role of Zfx in adult hematopoiesis (see below). Furthermore, Zfx^{null} ESC clones grew normally in short-term differentiation cultures without LIF (Fig. 3C,D) and expressed appropriate differentiation markers (Suppl. Fig. 3). Finally, Zfx^{null} ESC efficiently formed embryoid bodies (EB) that expressed the expected markers of hematopoietic differentiation (Keller, 2005) such as β-globin and Flk-1 (Fig. 3D,E and data not shown). These results suggest that the loss of Zfx impairs the self-renewal of undifferentiated ESC, but does not affect their developmental potential or the growth of their differentiated progeny.

In the course of these experiments, we noticed that ESC clones expressing higher levels of Zfx (Zfx^{null}+Zfx*, Fig. 2B) were less prone to differentiation. In short-term differentiation culture without LIF, Zfx-overexpressing ESC grew better than Zfx^{null} or Zfx^{flox} ESC (Fig. 3C) and retained undifferentiated phenotype (Fig. 3D), followed by massive cell death after re-plating. Furthermore, Zfx^{null}+Zfx* ESC generated small EB without cavities, which lost the pluripotency marker Nanog but failed to express hematopoietic differentiation marker β-globin (Fig. 3D,E). Finally, Zfx-overexpressing ESC failed to efficiently generate teratomas or mouse chimeras (data not shown). Thus, overexpression of Zfx appears to facilitate ESC self-renewal in sub-optimal conditions and to oppose ESC differentiation, the phenotype complementary to the loss of Zfx. Altogether, these data establish Zfx as a critical and specific regulator of ESC self-renewal.

Zfx is required for the self-renewal of adult HSC

To examine the role of Zfx in adult hematopoiesis, we generated Mx1-Cre^{+} Zfx^{flox}/y conditional knockout (CKO) mice, in which Cre-mediated Zfx deletion is induced by interferonogen pI·C (Kuhn et al., 1995). Two weeks after induction, total numbers of BM cells and of c-Kit^{+} Sca-1^{-} myeloid progenitors were unaffected in CKO mice, whereas the HSC-containing LSK population was significantly (P<0.0001) decreased (Fig. 4A). Time course analysis revealed a progressive loss of the HSC at 2–5 wk after induction, resulting in the decreased ratio of HSC to c-Kit^{+} Sca-1^{-} myeloid progenitors (Fig. 4B). The fractions of erythroid and myeloid differentiated cells were normal, while lymphocytes were initially depleted by pI·C treatment and failed to regenerate in the CKO BM (Suppl. Fig. 4). A similar loss of the LSK population was observed after Zfx deletion induced by tamoxifen-activated Cre construct (R26-CreER, Suppl. Fig. 5), ruling out potential side effects of pI·C injection.

The consequences of constitutive Zfx deletion in hematopoietic cells were analyzed using the Tie2-Cre strain, in which pan-hematopoietic Cre recombination is initiated in the early embryo (Koni et al., 2001). Zfx deletion was inefficient in most adult CKO mice, suggesting a strong selection against Zfx^{null} cells in adult hematopoiesis. Indeed, the rare adult CKO mice with a complete Zfx deletion (n=5) showed the same specific loss of the HSC population (Fig. 4C). In contrast, the CKO fetal livers were uniformly Zfx^{null} (Suppl. Fig. 2), exhibited normal cellularity and contained only a slightly reduced fraction of HSC (Fig. 4C). Furthermore, primitive hematopoiesis in the yolk sac of Zfx^{null} embryos was normal (Suppl. Fig. 6). Thus, the absence of Zfx abolishes the maintenance of adult BM HSC under steady-state conditions, but largely spares embryonic hematopoiesis.

Further analysis of the HSC/progenitor compartment in induced Mx1-Cre CKO mice (Fig. 4D) and in Tie2-Cre CKO mice (Suppl. Fig. 7) confirmed the loss of $Flt3^{-}$LSK subset that contains the self-renewing long-term HSC. In addition, the $Flt3^{+}$ LSK population containing short-term HSC and c-Kit^{low} $Flt3^{+}$ lymphoid progenitors including IL-7Rα^{+} common lymphoid progenitors (CLP) were severely reduced (Fig. 4D and Suppl. Fig. 4,5,7). The HSC in induced Mx1-Cre^{+} CKO mice proliferated normally, did not show increased egress from the BM, and displayed normal homing to and lodging in the BM after adoptive transfer (Suppl. Fig. 8). On the other hand, Zfx-deficient HSC showed a significant (P=0.0002) increase in Annexin V-

positive apoptotic cells (Fig. 4E). On the other hand, the Lin^{-} $Sca\text{-}1^{-}$ $c\text{-}Kit^{+}$ erythromyeloid progenitors were present in normal numbers, contained common and lineage-restricted subsets (Fig. 4D), did not show increased apoptosis (Fig. 4E) and maintained their characteristically high proliferation rate (Suppl. Fig. 8). Indeed, control and CKO BM generated similar numbers of erythroid and myeloid colonies in short-term colony-forming assays (Fig. 4F). These observations suggest that Zfx is required for the long-term survival of HSC but is dispensable in erythromyeloid progenitors.

Consistent with the defective maintenance of Zfx-deficient HSC, the BM from induced Mx1-Cre CKO mice failed to contribute to hematopoiesis in competitively reconstituted BM recipients (Fig. 5A,B). To measure the maintenance of HSC independent of their homing or engraftment, we induced the loss of Zfx in pre-established BM chimeric mice (Mikkola et al., 2003). Irradiated recipient mice ($CD45.1^{+}$ $CD45.2^{+}$) were transplanted with a mixture of donor BM from un-induced $Mx1\text{-}Cre^{+}$ CKO or control mice ($CD45.2^{+}$) and competitor wild-type BM ($CD45.1^{+}$). Four weeks later, chimeric mice were injected with pI·C to induce Zfx loss in the engrafted CKO BM, and the fraction of donor-derived peripheral blood leukocytes (PBL) was subsequently monitored (Fig. 5C). In contrast to all control recipient groups, the pI·C-injected recipients of CKO BM manifested a sharp decline of donor-derived PBL (Fig. 5D,E). The endpoint analysis 6 months after induction confirmed the virtual absence of Zfx-deficient donor cells in all hematopoietic cell types, including the HSC-containing LSK subset (Fig. 5F). These results demonstrate at the functional level that Zfx is absolutely required for the long-term HSC maintenance.

A common gene expression signature of Zfx-deficient SC

To identify Zfx target genes in SC, we compared global expression profiles of control and Zfx-deficient ESC and HSC. Several genes that were affected by Zfx loss in both ESC and HSC were identified, including 5 down-regulated genes (6 probes, P =0.0075) and 20 up-regulated genes (22 probes, $P=7 \times 10^{-8}$) (Fig. 6A and Suppl. Table I). In the latter group, a more permissive analysis suggested several additional candidates. By qPCR (Fig. 6B and Suppl. Table II), four down-regulated genes (*6720467C03Rik*, *AV340375*, *Phca* and *Retsat*) and six up-regulated genes (*Procr*, *Pkia*, *Ier3*, *Cryab*, *Gem* and *Ptgs2*) were validated as differentially expressed, revealing a common expression signature of Zfx-deficient ESC and HSC.

The predicted regulatory regions of commonly downregulated genes contain multiple potential binding sites for Zfx (Suppl. Fig. 9). To analyze the binding of Zfx to these genomic regions in live SC, we performed chromatin immunoprecipitation (ChIP) of epitope-tagged Zfx expressed in Zfx^{null} ESC (Zfx^{null}+Zfx^{TAG}, Suppl. Fig. 10). We found that promoter regions of *6720467C03Rik*, *AV340375* and *Retsat* were significantly enriched in ChIP with anti-tag antibodies; in contrast, no enrichment was seen in parental Zfx^{null} ESC that do not express tagged Zfx (Fig. 6C). Finally, the expression of all three genes was increased in Zfx-overexpressing ESC clones (Suppl. Table II). These results suggest that genes commonly downregulated in Zfx^{null} ESC and HSC are direct targets of Zfx.

Among the six genes coordinately up-regulated in Zfx-deficient ESC and HSC, four (*Cryab*, *Ier3*, *Gem* and *Ptgs2*) are known to be induced by stress, inflammatory stimuli and/or growth factors, with the latter three representing immediate-early genes. Therefore, their induction could be indirect and reflect the impaired function of Zfx-deficient SC. Indeed, four genes (*Pkia*, *Cryab*, *Ier3* and *Ptgs2*) were up-regulated in Zfx^{null} ESC and HSC, but not in their respective differentiated progeny (Fig. 6D). Notably, three genes (*Gem*, *Procr* and *Pkia*) display highly HSC-specific expression pattern ((Ivanova et al., 2002) and this study). The specific up-regulation of *Procr* in Zfx-deficient HSC was confirmed by cell surface staining for its product CD201 (Suppl. Fig. 11). Thus, the impaired self-renewal of Zfx-deficient ESC

and HSC correlates with SC-specific up-regulation of stress-inducible and/or immediate early genes.

Zfx controls ESC-specific regulators Tbx3 and Tcl1

To test whether Zfx controls genes and pathways specific only for a particular SC type, we analyzed known ESC-specific regulators of self-renewal. By protein staining (Suppl. Fig. 3), microarray analysis (Suppl. Table III) and qPCR (Fig. 7A), the components of the Nanog/Oct4/Sox2 transcriptional network were only minimally affected in Zfx^{null} ESC. On the other hand, we observed the downregulation of several ESC-specific genes including *Dub1/2*, *Ceacam1* and particularly *Tbx3*, which encodes a transcription factor required for ESC self-renewal (Ivanova et al., 2006). Further qPCR analysis showed that another ESC-specific regulator, *Tcl1*, was similarly reduced in Zfx^{null} ESC. Short-term batch culture of ESC after Cre-mediated Zfx deletion showed a prominent reduction of *Tbx3* and a slight decrease of *Tcl1*, but not of *Nanog* (Fig. 7B). Finally, Zfx-overexpressing ESC expressed higher levels of *Tbx3* and *Tcl1*, whereas *Nanog* and *Oct4* were unchanged (Fig. 7C).

The predicted promoter regions of *Tbx3* and *Tcl1* contain multiple consensus binding sites for Zfx (Suppl. Fig. 12). In the case of *Tbx3*, ChIP analysis localized the region of prominent Zfx binding to ~0.5 Kb upstream of the transcription start site (Fig. 7D). Indeed, the binding of Zfx to *Tbx3* and *Tcl1* promoters was detected only in Zfx-expressing Zfx^{null}+Zfx^{TAG} ESC, but not in the parental Zfx^{null} ESC (Fig. 7E). Finally, Zfx binding to *Tbx3* promoter was observed in undifferentiated ESC but not in ESC differentiated without LIF, consistent with the rapid loss of *Tbx3* expression upon differentiation (Fig. 7F). These data suggest that Zfx directly controls the expression of self-renewal regulators Tbx3 and Tcl1 in undifferentiated ESC.

Discussion

In this paper, we examined the biological role of *Zfx*, one of the first identified zinc finger-encoding genes (Schneider-Gadicke et al., 1989) whose properties and function remained unclear. We found that Zfx deletion impaired the growth of ESC *in vitro* and increased their apoptosis rate, particularly in defined serum-free conditions. Despite the growth and survival defect, Zfx-deficient ESC remained undifferentiated and gave rise to all lineages, including the germ line. Conversely, stable Zfx overexpression favored ESC self-renewal at the expense of differentiation. The requirement for Zfx in ESC self-renewal *in vitro* is not contradicted by the relatively normal early development of Zfx^{null} embryos, which survive until mid-gestation. Indeed, early embryonic development is not affected by the loss of several ESC self-renewal regulators such as Eras (Takahashi et al., 2003), Tcl1, Essrb or Tbx3 (Ivanova et al., 2006). Thus, our data suggest a critical role of Zfx in promoting ESC self-renewal, while it appears dispensable for ESC pluripotency.

In addition, we found that Zfx is not required for fetal hematopoiesis but essential in adult HSC, which failed to maintain their numbers or contribute to hematopoiesis after Zfx deletion. Zfx-deficient HSC interacted normally with their BM niche but showed an increase in apoptosis, suggesting a defect of long-term self-renewal due to impaired survival. In contrast, the survival and function of erythromyeloid progenitors were not affected, at least in the short term. Very similar phenotypes have been observed after the inducible deletion of Tel/Etv6 (Hock et al., 2004) or FoxO1/3/4 (Tothova et al., 2007), or after germ line deletion of Bmi-1 (Park et al., 2003) or Ikaros (Nichogiannopoulou et al., 1999) transcription factors. Similar to the latter three models, lymphopoiesis was severely impaired after the loss of Zfx. Thus, Zfx and possibly other HSC regulators appear to control both HSC self-renewal and lymphoid differentiation, but not erythromyeloid differentiation. Alternatively, the failure of lymphoid development might be secondary to defective HSC function, while erythromyeloid progenitors might be less dependent on HSC input (Nichogiannopoulou et al., 1999).

Although several transcriptional regulators were shown to control multiple SC types, the common regulation of ESC and adult SC has been difficult to demonstrate. For instance, *Polycomb group* (PcG) protein Bmi-1 promotes the self-renewal of HSC and of neural SC through the repression of *Cdkn2a* products $p16^{ink4a}$ and/or $p19^{Arf}$ (Lessard and Sauvageau, 2003;Molofsky et al., 2003;Park et al., 2003). On the other hand, ESC are resistant to $p16^{ink4a}$ and to other cyclin inhibitors (Burdon et al., 2002), and are not known to depend on Bmi-1. Conversely, PcG protein Eed contributes to the repression of differentiation-associated genes in ESC (Azuara et al., 2006;Boyer et al., 2006); however, Eed promotes proliferation and antagonizes Bmi-1 in hematopoietic cells (Lessard et al., 1999). In another case, transcription factor Sox2 controls the pluripotency of ESC and of neural stem/progenitor cells (Boyer et al., 2005;Graham et al., 2003;Ivanova et al., 2006). However, Sox2 is not expressed in other adult SC types, including HSC, and its specific role in adult neural SC remains to be established. Thus, Zfx provides a rare example of a transcription factor that is specifically required in ESC and in a canonical adult SC population such as the HSC.

Because the common transcriptional regulation of ESC and HSC has not been previously described, it is likely to be based on equally novel molecular mechanisms. Indeed, we have identified several direct target genes of Zfx in ESC and HSC, all of which are either predicted or poorly characterized. While the exact function of these direct Zfx targets is currently unknown, their coordinate regulation in ESC and HSC supports the common role of Zfx in these SC types. In addition, we identified several genes upregulated in Zfx-deficient ESC and HSC, likely as an indirect consequence of Zfx loss. Most of the coordinately induced genes are targets of stress, growth factor signaling and/or immediate-early response, suggesting that Zfx-deficient SC undergo excessive stress. This is consistent with increased apoptosis rate of Zfx^{null} ESC and HSC; furthermore, both immediate-early gene induction and decreased survival occur in undifferentiated ESC and HSC, but not in their differentiated progeny. Of note, HSC are uniquely sensitive to certain forms of stress such as physiological oxidative stress (Tothova et al., 2007). Altogether, our data reveal the apoptosis and concomitant upregulation of stress-inducible genes as common features of impaired self-renewal in ESC and HSC.

In addition to the common target genes, Zfx can directly activate cell type-specific targets, such as *Tbx3* and *Tcl1* in ESC. Both genes are rapidly downregulated upon ESC differentiation, and facilitate ESC self-renewal through a putative common pathway (Ivanova et al., 2006). Recently, Tcl1 was shown to control ESC growth but not their differentiation status (Matoba et al., 2006). Thus, Zfx may promote ESC self-renewal at least in part through the direct coordinate regulation of Tbx3 and Tcl1. Furthermore, the ESC-specific expression of Tbx3 and Tcl1 may partially explain the requirement for Zfx in ESC but not in their differentiated progeny. Although none of the known HSC regulators were affected by the loss of Zfx (Suppl. Table III and data not shown), Zfx may similarly regulate a yet unknown HSC-specific self-renewal pathway. At present, the ESC system provides a proof of principle that Zfx can control self-renewal pathways specific for a particular SC type.

In conclusion, our study has identified Zfx as a shared transcriptional regulator of two prototypical yet highly different murine SC types, the embryonic and hematopoietic SC. These results provide genetic evidence for a common molecular basis of self-renewal in pluripotent embryonic SC and adult tissue-specific SC. The identification of Zfx should facilitate the molecular dissection of self-renewal mechanisms in ESC, HSC and possibly in other SC types, including tumor-initiating cancer SC. Finally, the high evolutionary conservation of Zfx raises the possibility that it may regulate SC functions in other vertebrate species, including humans.

Experimental Procedures

Gene targeting

Conditional targeting, deletion and re-expression of Zfx in ESC were performed in male 129/SvEv ESC as described in Suppl. Fig. 1 and Suppl. Methods. The presence of Zfx protein was analyzed with an affinity-purified polyclonal antibody against the N-terminal domain. Zfx^{flox} and Zfx^{null} ESC clones were injected into C57BL/6 blastocysts, and the resulting chimeric males were crossed to wild-type 129/SvEv and Black Swiss females, respectively.

To obtain CKO mice (Zfx^{flox}/y, Cre^{+}), $Zfx^{flox/flox}$ females (pure 129/SvEv background) were crossed with males carrying Mx1-Cre (129/SvEv) or Tie2-Cre (mixed 129/B6) transgenes. Control mice in both strains included Cre^{+} wild-type and $Cre^{-}Zfx^{flox}$/y animals, which were indistinguishable by all assays. Mice carrying a tamoxifen-inducible Cre recombinase inserted into *Rosa26* locus (R26-CreER, C57BL/6) were kindly provided by Dr. Thomas Ludwig, Columbia University. The recombination in adult Mx1-Cre mice was induced with polyinosinic:polycytidylic acid (pI·C, Amersham Biosciences) administered i.p. three times (0.25 mg every third day). The deletion status of all analyzed CKO cells and tissues was monitored by genomic PCR. All animal studies were performed according to the investigator's protocol approved by the Institutional Animal Care and Use Committee.

Cell Culture and Analysis

Undifferentiated ESC were cultured in complete DMEM containing 15% FCS and recombinant LIF (Chemicon) on mitomycin-treated embryonic fibroblast feeders. For gene expression studies and ChIP, ESC were grown on gelatin-coated plates in 5–15% Knockout SR serum replacement (Invitrogen) and LIF. Serum- and feeder-free culture in the presence of LIF and 10 ng/ml recombinant BMP4 (R&D Systems) was performed as described (Ying et al., 2003). To measure cell growth or colony formation, ESC were seeded into triplicate wells of 24-well plates and cultured as indicated. Apoptosis of ESC was measured by gel fractionation of low molecular weight DNA or by staining live cells with Annexin V-FITC conjugate (BD Pharmingen) and 7-amino-actinomycin D (7-AAD). For competitive growth assay, $Zfx^{flox\text{-}neo}$ ESC were transiently transfected with Cre expression vector and grown as indicated. For the batch culture of Zfx^{null} ESC shortly after Zfx deletion, $Zfx^{flox\text{-}neo}$ ESC were transiently transfected with Cre-GFP expression vector, and GFP^{+} cells were sorted 24 hrs later and cultured for 3 days with LIF on gelatin. Control ESC were generated in parallel by transfection with an empty expression vector.

For differentiation, ESC were grown in 15% FCS without LIF/feeders on gelatin-coated plates. Where indicated, ESC were cultured in suspension for 4 days to form primitive embryoid bodies (EB), and then returned to adherent culture or allowed to form mature EB in suspension for additional 4–9 days. For teratoma formation, undifferentiated ESC grown on gelatin were injected s.c. into syngeneic 129/SvEv mice, and teratomas were harvested 3 weeks later, sectioned and stained with hematoxylin-eosin.

Mouse embryonic fibroblasts (MEF) were derived from 14.5 d.p.c. R26-$CreER^{+}$, Zfx^{flox}/y embryos. After the first passage, half of the culture was incubated with 4-hydroxytamoxifen to induce Zfx deletion, and then equal numbers of treated and untreated cells were mixed and propagated by the 3T3 protocol.

Hematopoietic cell analysis

Single-cell suspensions from hematopoietic organs were stained with the indicated fluorochrome-conjugated antibodies (BD Pharmingen and eBiosciences) for 4-or 5-color analysis. The lineage cocktail included antibodies to CD11b, Gr-1, Ter119, B220, CD3 and

DX5. For apoptosis detection, enriched lineage-negative BM cells were stained with antibody conjugates, Annexin V TACS reagent (Trevigen) and 7-AAD. The samples were acquired using FACSCalibur or LSR II flow cytometers or sorted on FACSAria flow sorter (BD Immunocytometry Systems), and analyzed using FlowJo software (Treestar Inc.). Statistical significance was estimated using unpaired, two-tailed Student's *t*-test. For competitive reconstitution, BM cells from control (Mx1-Cre$^+$) or CKO (*Zfx*^{flox}/y, Mx1-Cre$^+$) mice 7 days after pI·C injection was mixed 2:1 with the competitor BM cells from B6.SJL mice (C57BL/6 congenic for CD45.1), and 2x10^6 total cells were injected i.v. into lethally irradiated B6.SJL recipients. For Zfx deletion in pre-established BM chimeras, BM cells from untreated Mx1-Cre$^+$ control or CKO mice were mixed 2:1 with competitor B6.SJL BM and injected i.v. into lethally irradiated (129/SvEv x B6.SJL)F1 recipients. Four weeks later, one half of each recipient group was treated with pI·C. For progenitor assays, total BM was plated in triplicates (10^5 cells/35 mm dish) into cytokine-supplemented methylcellulose medium (Methocult, Stem Cell Technologies), and the number and morphology of colonies were scored 10 days later.

Global gene expression analysis

For ESC, *Zfx*^{null} and control *Zfx*^{flox} clones were grown on gelatin in medium with 15% Knockout SR and LIF. For HSC, BM cells were pooled from 4–6 Mx1-Cre$^+$ *Zfx*^{flox}/y CKO and control *Zfx*^{flox}/y Cre$^-$ littermates 4 days after the last pI·C injection, and Lin$^-$Sca-1$^+$ c-Kit$^+$ cells were flow-sorted. RNA was amplified, labeled and hybridized to Mouse Genome 430 2.0 microarrays containing probes for ~37,000 genes (Affymetrix). Details of the sample preparation and analysis are described in Suppl. Methods. Microarray data have been deposited in the GEO database under accession number GSE7069.

Quantitative PCR

Total cell RNA was reverse-transcribed and assayed by quantitative real-time PCR using SYBR Green incorporation. The expression of all genes was normalized to that of β-actin and expressed relative to the indicated reference sample (average ± S.D. of triplicate reactions). For competition experiments (Fig. 2A), *Zfx*^{flox} and *Zfx*^{null} alleles were amplified separately and normalized using qPCR reaction that detects all targeted *Zfx* alleles but not the feeder cell-derived wild-type allele. The measurements of *Zfx* expression (Fig. 1A) were performed using the calibration curve method. All other cDNA and genomic DNA measurements were performed using the $\Delta\Delta C_T$ method on MX3000P instrument (Stratagene).

Chromatin Immunoprecipitation (ChIP)

An ESC clone expressing FLAG-HA epitope-tagged Zfx protein (Zfx-TAG) was generated as described in Suppl. Methods. Zfx-TAG cells or parental *Zfx*^{null} cells were crosslinked with formaldehyde and subjected to ChIP using anti-FLAG M2 antibody (Sigma) or control IgG as described (Boyer et al., 2005). After crosslink reversal, precipitated chromatin was analyzed by qPCR for genomic fragments of interest. For experiments shown in Fig. 7E, ChIP was performed using anti-Zfx antibody or control IgG, followed by whole genome ligation-mediated PCR amplification as described (Boyer et al., 2005). All results were normalized using a control genomic DNA fragment from murine *Snai3* gene, which was not enriched in Zfx ChIP.

Supplementary Material

Refer to Web version on PubMed Central for supplementary material.

Acknowledgements

We thank Philip Leder for his invaluable support of these studies, David C. Page and Mary Goodheart for encouragement and helpful discussions, T. Palomero and A. Ferrando for advice on ChIP, and T. Ludwig, C. Troy,

H. Wichterle, C. Schindler, C. Henderson and H. Gu for reagents and access to instrumentation. Supported in part by the NIH grant HL084353, American Cancer Society grant RSG-06-149-01 and the March of Dimes Foundation Basil O'Connor Starting Scholar Award 5-FY04-23 to B.R., and by the NRSA awards AI007525 and AI066459 to T.L.A.

References

Azuara V, Perry P, Sauer S, Spivakov M, Jorgensen HF, John RM, Gouti M, Casanova M, Warnes G, Merkenschlager M, Fisher AG. Chromatin signatures of pluripotent cell lines. Nat Cell Biol 2006;8:532–538. [PubMed: 16570078]

Boiani M, Scholer HR. Regulatory networks in embryo-derived pluripotent stem cells. Nat Rev Mol Cell Biol 2005;6:872–884. [PubMed: 16227977]

Boyer LA, Lee TI, Cole MF, Johnstone SE, Levine SS, Zucker JP, Guenther MG, Kumar RM, Murray HL, Jenner RG, et al. Core transcriptional regulatory circuitry in human embryonic stem cells. Cell 2005;122:947–956. [PubMed: 16153702]

Boyer LA, Plath K, Zeitlinger J, Brambrink T, Medeiros LA, Lee TI, Levine SS, Wernig M, Tajonar A, Ray MK, et al. Polycomb complexes repress developmental regulators in murine embryonic stem cells. Nature 2006;441:349–353. [PubMed: 16625203]

Burdon T, Smith A, Savatier P. Signalling, cell cycle and pluripotency in embryonic stem cells. Trends Cell Biol 2002;12:432–438. [PubMed: 12220864]

Calvi LM, Adams GB, Weibrecht KW, Weber JM, Olson DP, Knight MC, Martin RP, Schipani E, Divieti P, Bringhurst FR, et al. Osteoblastic cells regulate the haematopoietic stem cell niche. Nature 2003;425:841–846. [PubMed: 14574413]

Chambers I, Smith A. Self-renewal of teratocarcinoma and embryonic stem cells. Oncogene 2004;23:7150–7160. [PubMed: 15378075]

Cheng T, Rodrigues N, Shen H, Yang Y, Dombkowski D, Sykes M, Scadden DT. Hematopoietic stem cell quiescence maintained by p21cip1/waf1. Science 2000;287:1804–1808. [PubMed: 10710306]

D'Amour KA, Gage FH. Genetic and functional differences between multipotent neural and pluripotent embryonic stem cells. Proc Natl Acad Sci U S A 2003;100(Suppl 1):11866–11872. [PubMed: 12923297]

Eckfeldt CE, Mendenhall EM, Verfaillie CM. The molecular repertoire of the 'almighty' stem cell. Nat Rev Mol Cell Biol 2005;6:726–737. [PubMed: 16103873]

Fortunel NO, Otu HH, Ng HH, Chen J, Mu X, Chevassut T, Li X, Joseph M, Bailey C, Hatzfeld JA, et al. Comment on " 'Stemness': transcriptional profiling of embryonic and adult stem cells" and "a stem cell molecular signature". Science 2003;302:393. 393. [PubMed: 14563990]author reply

Graham V, Khudyakov J, Ellis P, Pevny L. SOX2 functions to maintain neural progenitor identity. Neuron 2003;39:749–765. [PubMed: 12948443]

Hock H, Meade E, Medeiros S, Schindler JW, Valk PJ, Fujiwara Y, Orkin SH. Tel/Etv6 is an essential and selective regulator of adult hematopoietic stem cell survival. Genes Dev 2004;18:2336–2341. [PubMed: 15371326]

Ivanova N, Dobrin R, Lu R, Kotenko I, Levorse J, DeCoste C, Schafer X, Lun Y, Lemischka IR. Dissecting self-renewal in stem cells with RNA interference. Nature 2006;442:533–538. [PubMed: 16767105]

Ivanova NB, Dimos JT, Schaniel C, Hackney JA, Moore KA, Lemischka IR. A stem cell molecular signature. Science 2002;298:601–604. [PubMed: 12228721]

Keller G. Embryonic stem cell differentiation: emergence of a new era in biology and medicine. Genes Dev 2005;19:1129–1155. [PubMed: 15905405]

Kondo M, Wagers AJ, Manz MG, Prohaska SS, Scherer DC, Beilhack GF, Shizuru JA, Weissman IL. BIOLOGY OF HEMATOPOIETIC STEM CELLS AND PROGENITORS: Implications for Clinical Application. Annu Rev Immunol 2003;21:759–806. [PubMed: 12615892]

Koni PA, Joshi SK, Temann UA, Olson D, Burkly L, Flavell RA. Conditional vascular cell adhesion molecule 1 deletion in mice: impaired lymphocyte migration to bone marrow. J Exp Med 2001;193:741–754. [PubMed: 11257140]

Kuhn R, Schwenk F, Aguet M, Rajewsky K. Inducible gene targeting in mice. Science 1995;269:1427–1429. [PubMed: 7660125]

Lessard J, Sauvageau G. Bmi-1 determines the proliferative capacity of normal and leukaemic stem cells. Nature 2003;423:255–260. [PubMed: 12714970]

Lessard J, Schumacher A, Thorsteinsdottir U, van Lohuizen M, Magnuson T, Sauvageau G. Functional antagonism of the Polycomb-Group genes eed and Bmi1 in hemopoietic cell proliferation. Genes Dev 1999;13:2691–2703. [PubMed: 10541555]

Li L, Xie T. Stem cell niche: structure and function. Annu Rev Cell Dev Biol 2005;21:605–631. [PubMed: 16212509]

Luoh SW, Bain PA, Polakiewicz RD, Goodheart ML, Gardner H, Jaenisch R, Page DC. Zfx mutation results in small animal size and reduced germ cell number in male and female mice. Development 1997;124:2275–2284. [PubMed: 9187153]

Matoba R, Niwa H, Masui S, Ohtsuka S, Carter MG, Sharov AA, Ko MS. Dissecting oct3/4-regulated gene networks in embryonic stem cells by expression profiling. PLoS ONE 2006;1:e26. [PubMed: 17183653]

Mikkers H, Frisen J. Deconstructing stemness. Embo J 2005;24:2715–2719. [PubMed: 16037819]

Mikkola HK, Klintman J, Yang H, Hock H, Schlaeger TM, Fujiwara Y, Orkin SH. Haematopoietic stem cells retain long-term repopulating activity and multipotency in the absence of stem-cell leukaemia SCL/tal-1 gene. Nature 2003;421:547–551. [PubMed: 12540851]

Molofsky AV, Pardal R, Iwashita T, Park IK, Clarke MF, Morrison SJ. Bmi-1 dependence distinguishes neural stem cell self-renewal from progenitor proliferation. Nature 2003;425:962–967. [PubMed: 14574365]

Nichogiannopoulou A, Trevisan M, Neben S, Friedrich C, Georgopoulos K. Defects in hemopoietic stem cell activity in Ikaros mutant mice. J Exp Med 1999;190:1201–1214. [PubMed: 10544193]

Park IK, Qian D, Kiel M, Becker MW, Pihalja M, Weissman IL, Morrison SJ, Clarke MF. Bmi-1 is required for maintenance of adult self-renewing haematopoietic stem cells. Nature 2003;423:302–305. [PubMed: 12714971]

Ramalho-Santos M, Yoon S, Matsuzaki Y, Mulligan RC, Melton DA. "Stemness": transcriptional profiling of embryonic and adult stem cells. Science 2002;298:597–600. [PubMed: 12228720]

Sakaguchi T, Nishimoto M, Miyagi S, Iwama A, Morita Y, Iwamori N, Nakauchi H, Kiyonari H, Muramatsu M, Okuda A. Putative "stemness" gene jam-B is not required for maintenance of stem cell state in embryonic, neural, or hematopoietic stem cells. Mol Cell Biol 2006;26:6557–6570. [PubMed: 16914739]

Schneider-Gadicke A, Beer-Romero P, Brown LG, Mardon G, Luoh SW, Page DC. Putative transcription activator with alternative isoforms encoded by human ZFX gene. Nature 1989;342:708–711. [PubMed: 2512506]

Takahashi K, Mitsui K, Yamanaka S. Role of ERas in promoting tumour-like properties in mouse embryonic stem cells. Nature 2003;423:541–545. [PubMed: 12774123]

Takahashi K, Yamanaka S. Induction of pluripotent stem cells from mouse embryonic and adult fibroblast cultures by defined factors. Cell 2006;126:663–676. [PubMed: 16904174]

Tothova Z, Kollipara R, Huntly BJ, Lee BH, Castrillon DH, Cullen DE, McDowell EP, Lazo-Kallanian S, Williams IR, Sears C, et al. FoxOs are critical mediators of hematopoietic stem cell resistance to physiologic oxidative stress. Cell 2007;128:325–339. [PubMed: 17254970]

Wang J, Rao S, Chu J, Shen X, Levasseur DN, Theunissen TW, Orkin SH. A protein interaction network for pluripotency of embryonic stem cells. Nature 2006;444:364–368. [PubMed: 17093407]

Weissman IL, Anderson DJ, Gage F. Stem and progenitor cells: origins, phenotypes, lineage commitments, and transdifferentiations. Annu Rev Cell Dev Biol 2001;17:387–403. [PubMed: 11687494]

Yilmaz OH, Valdez R, Theisen BK, Guo W, Ferguson DO, Wu H, Morrison SJ. Pten dependence distinguishes haematopoietic stem cells from leukaemia-initiating cells. Nature 2006;441:475–482. [PubMed: 16598206]

Ying QL, Nichols J, Chambers I, Smith A. BMP induction of Id proteins suppresses differentiation and sustains embryonic stem cell self-renewal in collaboration with STAT3. Cell 2003;115:281–292. [PubMed: 14636556]

Zhang J, Grindley JC, Yin T, Jayasinghe S, He XC, Ross JT, Haug JS, Rupp D, Porter-Westpfahl KS, Wiedemann LM, et al. PTEN maintains haematopoietic stem cells and acts in lineage choice and leukaemia prevention. Nature 2006;441:518–522. [PubMed: 16633340]

Zhang J, Niu C, Ye L, Huang H, He X, Tong WG, Ross J, Haug J, Johnson T, Feng JQ, et al. Identification of the haematopoietic stem cell niche and control of the niche size. Nature 2003;425:836–841. [PubMed: 14574412]

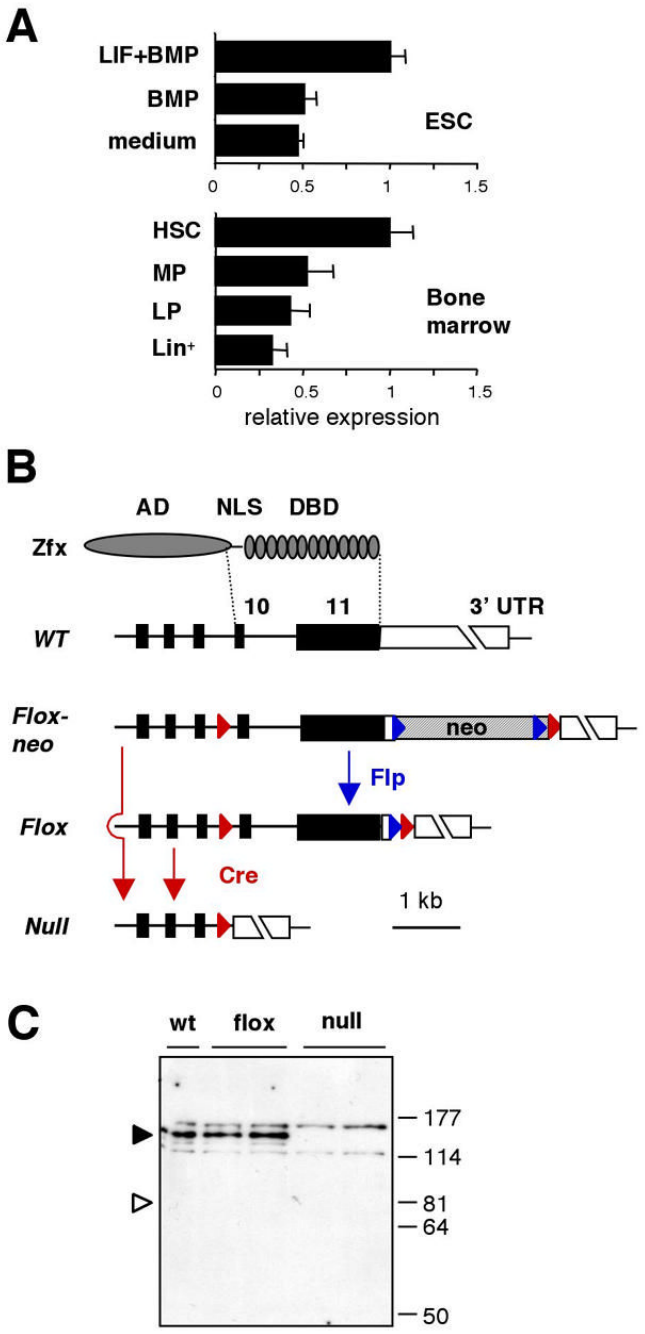

Figure 1. The expression analysis and conditional targeting of Zfx

(A) The expression of *Zfx* is elevated in undifferentialed murine ESC and HSC. The ESC were grown in serum-free culture with LIF+BMP4 (undifferentiated), BMP4 or medium alone (differentiated). Wild-type BM was sorted into lineage-positive (Lin^+) differentiated cells and Lin^- populations including HSC ($Sca\text{-}1^+$ $c\text{-}Kit^+$), myeloid progenitors (MP, $Sca\text{-}1^-$ $c\text{-}Kit^+$) and lymphoid progenitors (LP, $Sca\text{-}1^{low}$ $c\text{-}Kit^{low}$). Shown is normalized *Zfx* expression relative to the corresponding SC sample as measured by qPCR. **(B)** The strategy of *Zfx* gene targeting. Exons 10 and 11 encoding the NLS and DBD of Zfx protein were flanked by *LoxP* sites (red triangles). The neomycin resistance (neo) cassette flanked by *FRT* sites (blue triangles) was excised from the targeted $Zfx^{flox\text{-}neo}$ allele by Flp-mediated recombination. Cre-mediated

recombination of either $Zfx^{flox\text{-}neo}$ or Zfx^{flox} allele produces the Zfx^{null} allele. **(C)** The expression of Zfx protein in the wild-type (wt) or targeted ESC clones, analyzed by Western blotting with antibodies against Zfx N-terminal AD. The positions of full-length Zfx and of the predicted protein encoded by the null allele (determined using the corresponding epitope-tagged expression constructs) are indicated by filled and open triangles, respectively.

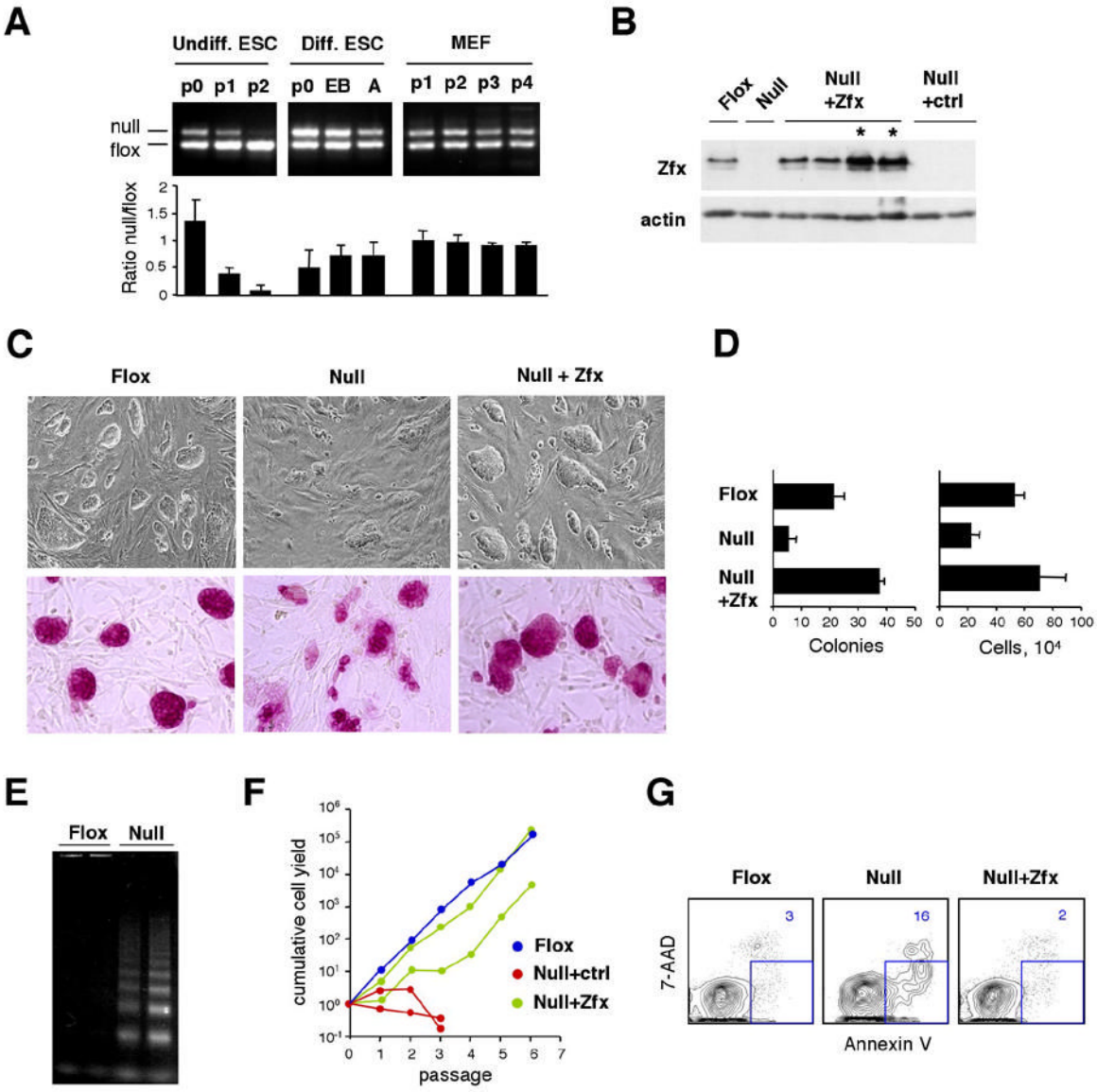

Figure 2. Defective self-renewal of Zfx-deficient ESC

(A) Impaired competitive growth of Zfx-deficient ESC but not of differentiated cells. Cre recombination was transiently induced in ESC or in primary embryonic fibroblasts (MEF), and the presence of Zfx^{null} cells at subsequent passages (P) was monitored by genomic PCR. The ESC were grown in serum/LIF/feeders (undiff.) or differentiated (diff.) into primitive embryoid bodies (EB) followed by adherent culture (A). Shown are the simultaneous amplification of Zfx^{null} and Zfx^{flox} alleles and the ratios of separately amplified alleles determined by qPCR. **(B)** Re-expression of Zfx in Zfx-deficient ESC. Zfx^{null} ESC stably transfected with Zfx or control constructs (ctrl) were analyzed by Western blotting with anti-Zfx Ab. The clones overexpressing Zfx are indicated with an asterisk. **(C)** Defective colony morphology of Zfx-deficient ESC. Shown are live cultures (magnification 100x) and fixed cells stained for alkaline phosphatase (purple, magnification 200x) of ESC grown with serum/LIF/feeders. **(D)** Defective growth and colony forming capacity of Zfx-deficient ESC clones in serum/LIF/feeders. Shown are numbers of colonies and total cell yields of ESC (average ± S.D. of triplicate cultures) after one passage at single-cell (10^2/well) or regular (10^4/well) densities, respectively.

(E) Increased apoptosis of Zfx-deficient ESC clones grown in serum/LIF, as measured by DNA laddering assay (two clones per genotype). **(F)** Defective growth of Zfx-deficient ESC clones in serum-free culture with LIF+BMP4. The data represent average cell yields of parallel triplicate cultures for each clone. **(G)** Increased apoptosis of Zfx-deficient ESC in serum-free culture. After one passage in LIF+BMP4, cells were stained for Annexin V and DNA content (7-AAD); the fraction of $Annexin^{+}$ $7\text{-}AAD^{-}$ apoptotic cells is indicated.

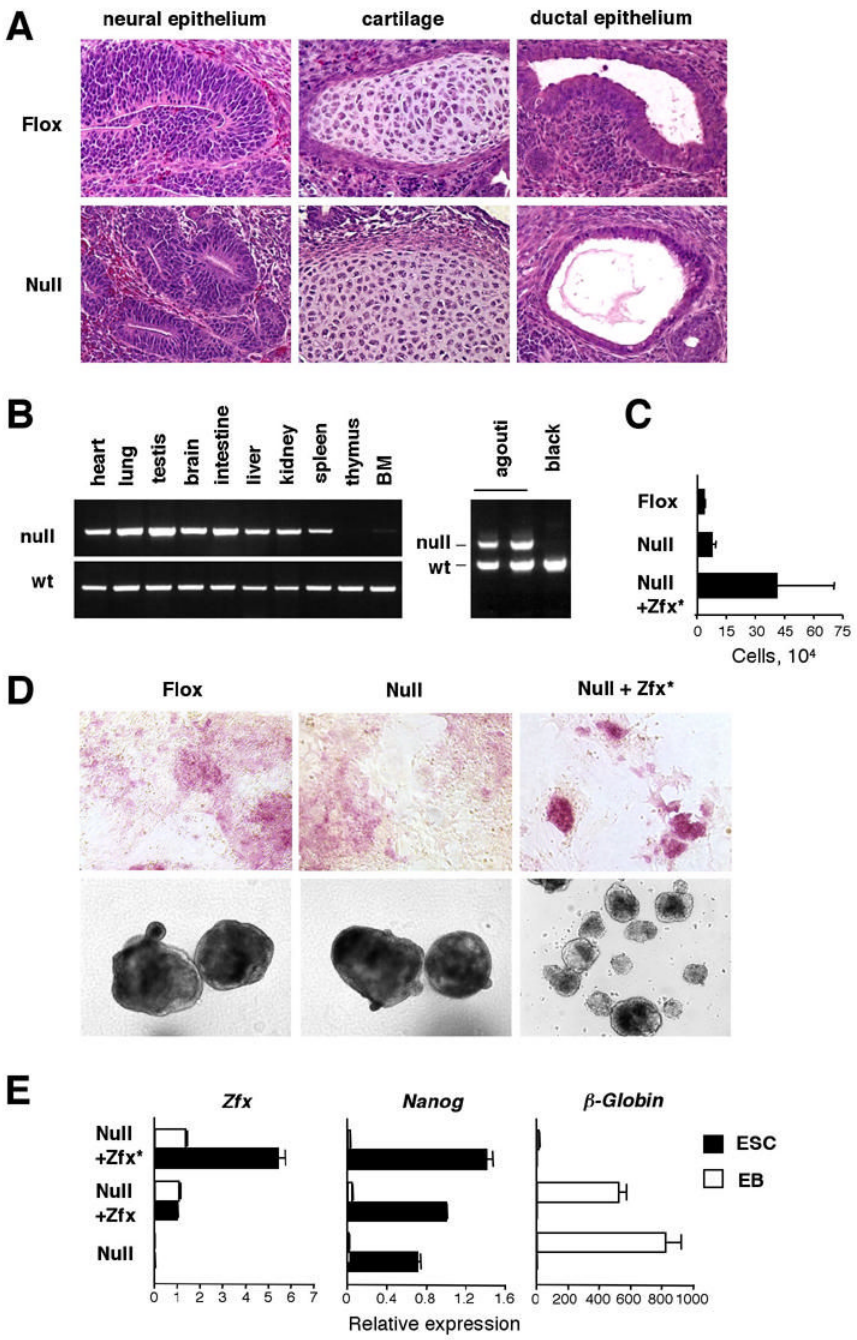

Figure 3. Normal differentiation capacity of Zfx-deficient ESC

(A) Normal teratoma formation by control (Zfx^{flox}) and Zfx^{null} ESC clones (representative of two clones per genotype). Differentiated tissues in hematoxylin/eosin-stained sections of teratomas are shown (magnification 200x). **(B)** The contribution of Zfx^{null} ESC to tissues of chimeric mice. Left panel: null and wild-type Zfx alleles were separately amplified from genomic DNA of chimeric mouse tissues (representative of three chimeras). Right panel: female progeny of a chimeric mouse were genotyped, confirming germ line transmission of Zfx^{null} allele. **(C)** The growth in differentiating conditions of ESC clones lacking (Zfx^{null}) or overexpressing (Zfx^{null}+Zfx*) Zfx. Shown are average cell yields of triplicate cultures plated at $2x10^4$/well and grown for one passage without LIF or feeders. **(D)** The same ESC clones

were grown without LIF and stained for alkaline phosphatase (purple, upper panel) or induced to form mature EB (lower panel). Magnification, 100x. **(E)** The expression of pluripotency (*Nanog*) and differentiation (*β-globin*) markers in undifferentiated ESC or in EB measured by qPCR relative to the expression in Zfx^{null}+Zfx ESC.

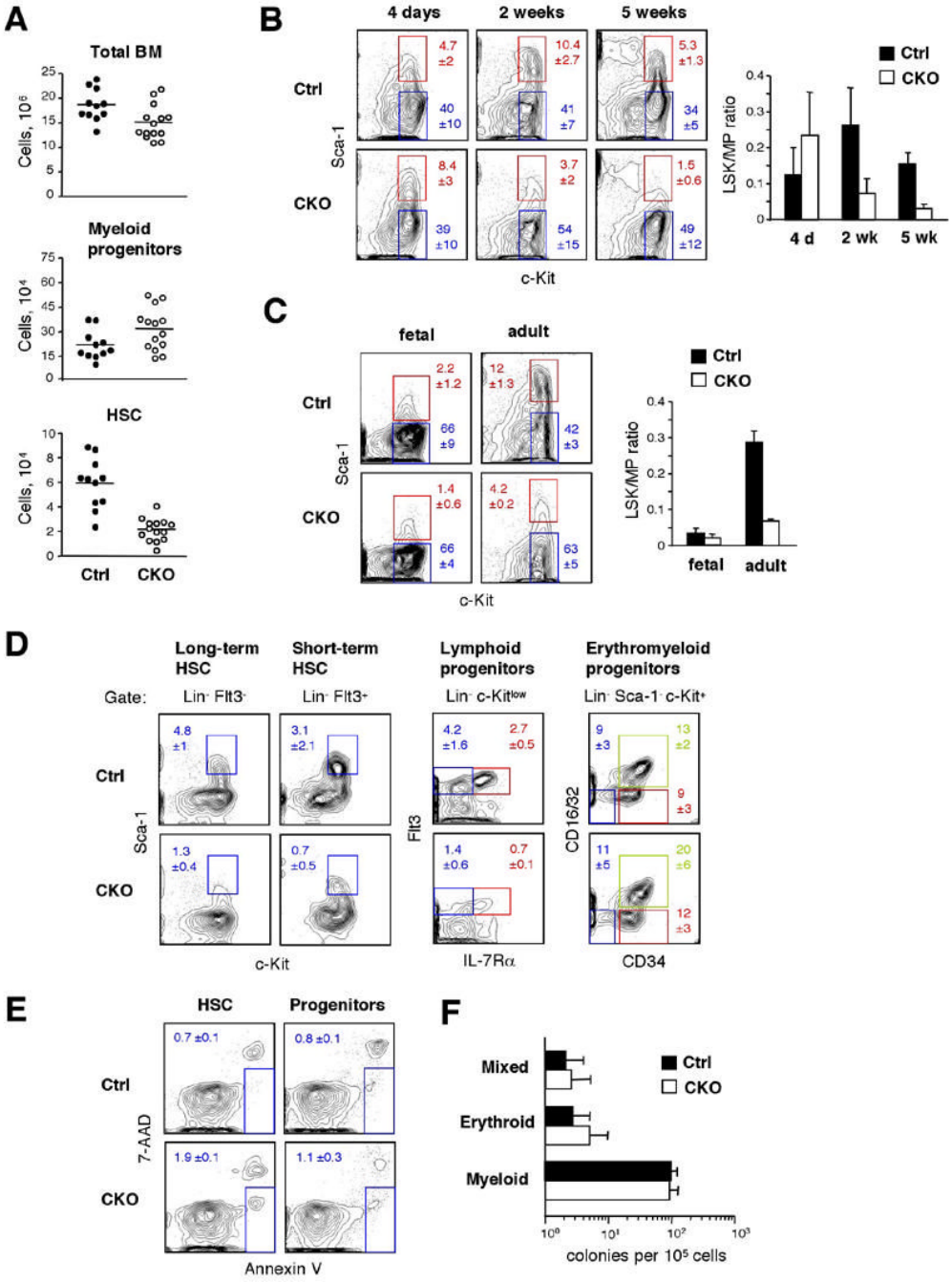

Figure 4. The loss of adult HSC after Zfx deletion in hematopoietic cells

(A) The decrease in HSC numbers after Zfx deletion from the BM. Shown are absolute numbers of total BM cells, myeloid progenitors and the HSC-containing LSK population in control and Mx1-Cre^{+} *Zfx*^{flox}/y CKO mice two weeks after pI·C injection. Each symbol represents an individual mouse. **(B)** The loss of HSC from the stem/progenitor compartment of Mx1-Cre^{+} CKO BM at the indicated times after pI·C injection. Shown are the staining profiles of Lin^{-} cells, with the LSK population (red) and erythromyeloid progenitors (blue) and their percentages indicated (average ± S.D. of 3–12 animals). The graph shows average ratios of the LSK to myeloid progenitor fractions. **(C)** The loss of adult HSC after constitutive Zfx deletion in the hematopoietic system. The HSC and myeloid progenitor populations in the fetal liver

(n=6–9) or in adult BM (n=4–5) of Tie2-Cre^{+} CKO and control mice are shown as in panel B. **(D)** Decreased HSC and lymphoid progenitors but normal myeloid progenitors in Mx1-Cre^{+} CKO mice two weeks after pI·C injection. Shown are Flt3^{-} and Flt3^{+} LSK populations containing long-term and short-term HSC, respectively; Flt3^{+} Lin^{-} c-Kit^{low} lymphoid progenitors including the IL-7Rα_{+} CLP subset (red); and Lin^{-} Sca-1^{-} c-Kit^{+} erythromyeloid progenitors divided into common myeloid progenitor (red), erythrocyte/megakaryocyte progenitor (blue) and granulocyte/monocyte progenitor (green). The fraction of each subset in the Lin^{-}population is indicated (average ± S.D. of 5 animals). **(E)** Increased HSC apoptosis in Mx1-Cre^{+} CKO mice two weeks after pI·C injection. Shown are gated HSC (the LSK subset) and erythromyeloid progenitors (Lin^{-} Sca-1^{-} c-Kit^{+}) stained for Annexin V and DNA content (7-AAD). The fractions of Annexin^{+} 7-AAD^{-} apoptotic cells (highlighted) are indicated (average ± S.D. of 3 animals). **(F)** Normal erythromyeloid progenitor function in Zfx-deficient BM. Shown is *in vitro* colony formation by BM cells from Mx1-Cre^{+} CKO or control mice two weeks after pI·C injection (average ± S.D. of 4 animals).

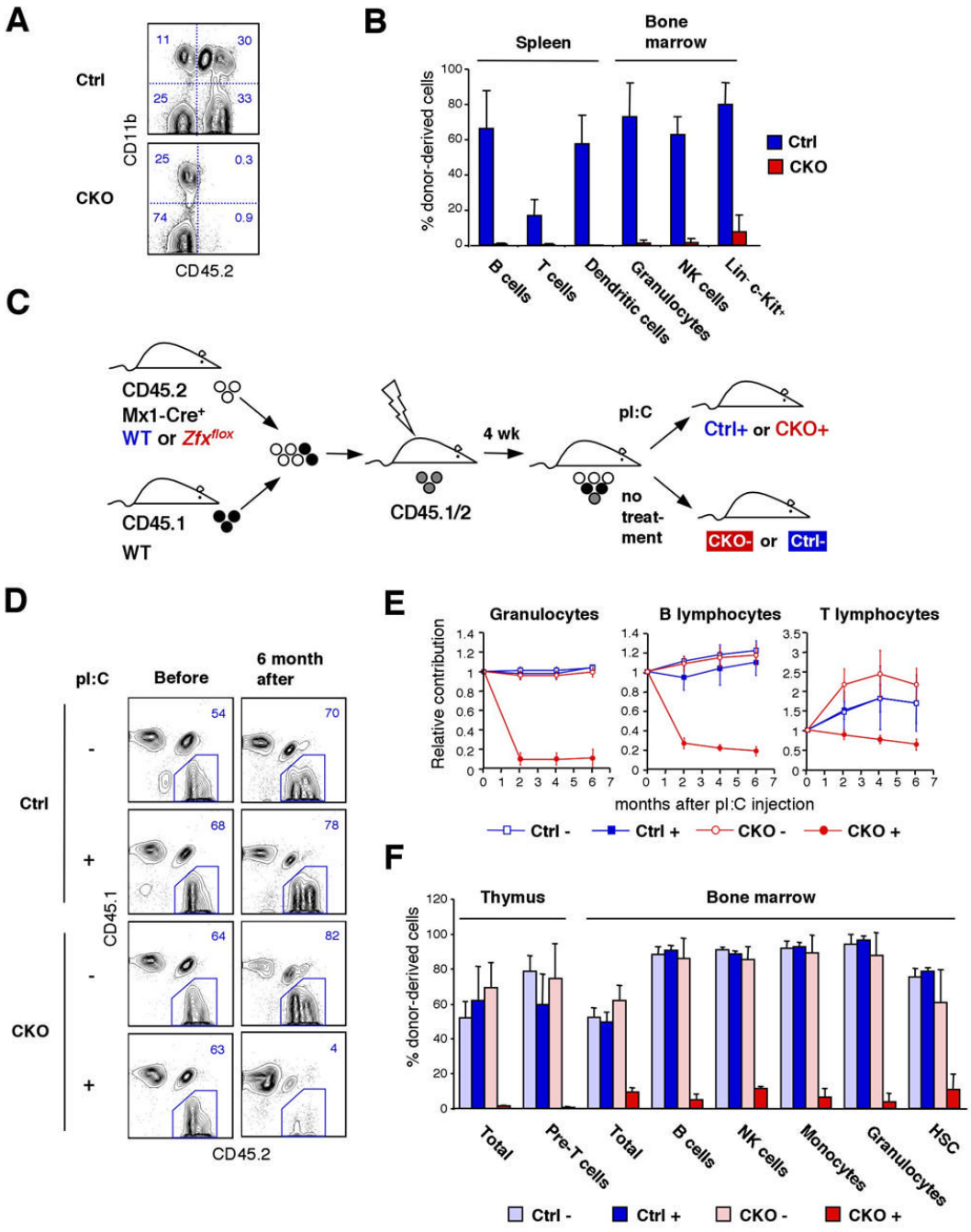

Figure 5. The loss of Zfx abolishes HSC function

(A-B) Defective hematopoietic reconstitution by Zfx-deficient BM. Control or Mx1-Cre$^+$ CKO mice (CD45.2$^+$) were injected with pI·C to induce Zfx deletion, and their BM was mixed with wild-type competitor BM (CD45.1$^+$) and transferred into irradiated CD45.1$^+$ recipients. Shown are representative staining profiles of PBL **(A)** and the fractions of donor-derived CD45.2$^+$ cells in the indicated lineages **(B)** two months after BM transfer (average ± S.D. of 3 recipients). **(C-F)** The loss of HSC maintenance after Zfx deletion in pre-established BM chimeras. **(C)** Experimental strategy. **(D)** Representative staining profiles of total PBL in the recipient mice before or 6 months after pI·C injection, showing donor (CD45.2$^+$CD45.1$^-$, highlighted), competitor (CD45.2$^-$CD45.1$^+$) and residual host (CD45.2$^+$CD45.1$^+$) cells. **(E)** Relative

contribution of donor-derived cells to major PBL lineages over time. The donor-derived fraction before pI·C injection (>50% in all mice) was taken as one for each recipient; the data represent average ± S.D. of 4 recipients per group. A representative of 3 independent reconstitution experiments is shown. **(F)** The percentage of donor-derived cells in the indicated cell subsets in the thymus and BM 6 months after pI·C injection.

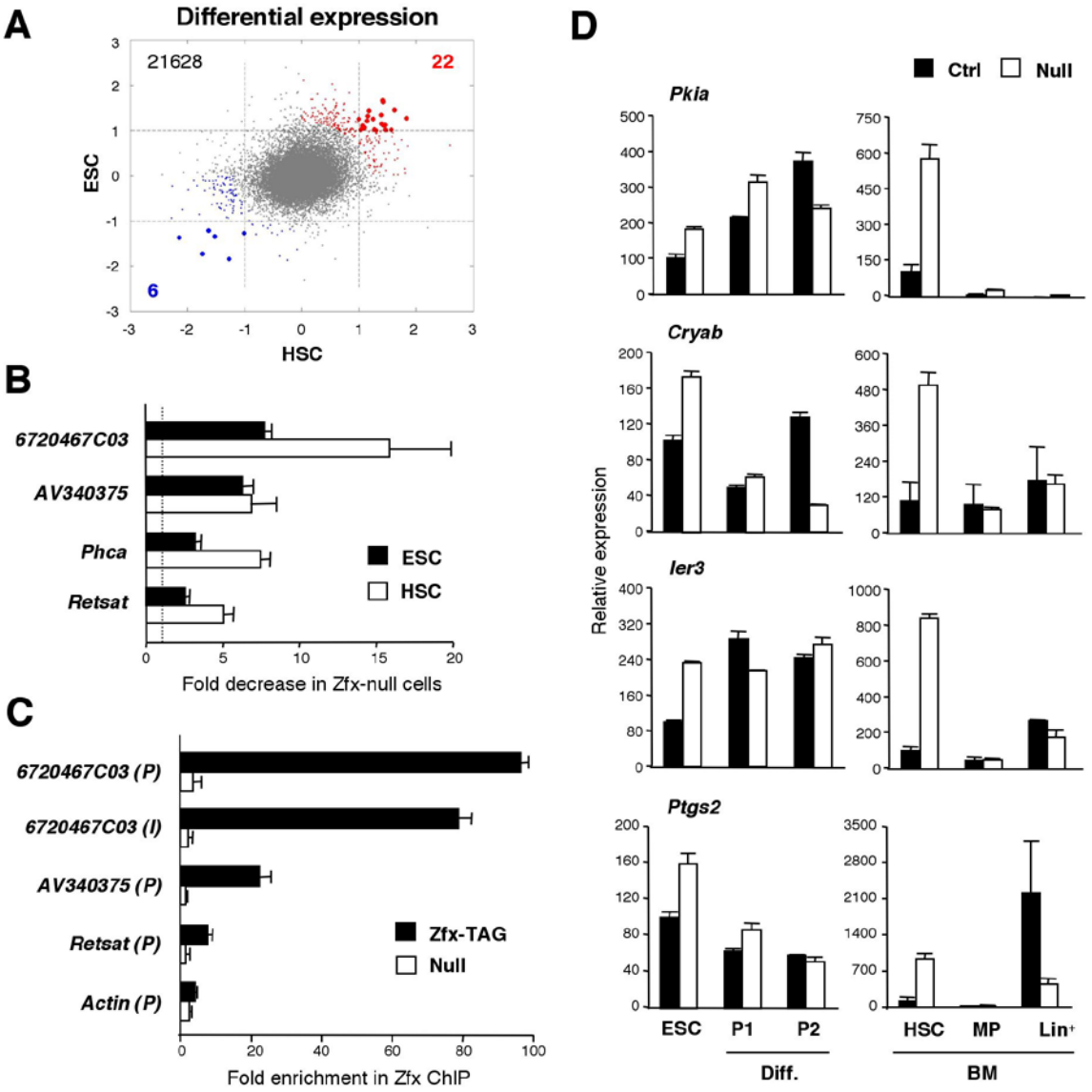

Figure 6. A common gene expression signature of Zfx-deficient ESC and HSC

(A) Genome-wide expression analysis of Zfx-deficient ESC and HSC using microarrays. Data points represent normalized increase (>0) or decrease (<0) in individual probe levels in Zfx^{null} ESC and HSC relative to the respective controls. Probes showing coordinated decrease or increase in Zfx^{null} ESC and HSC are indicated as large blue and red dots, respectively; small colored dots represent a more permissive analysis. The numbers of total and coordinately changing probes are indicated. **(B)** The down-regulation of common target genes in HSC and ESC after Zfx deletion. HSC were sorted from control and Mx1-Cre^{+} CKO BM 4 days after pI·C injection. Short-term batch cultures of Zfx^{null} ESC were generated by sorting $Zfx^{flox\text{-}neo}$ ESC transfected with Cre-GFP. The data represent fold decrease of the indicated transcripts in Zfx^{null} over control SC as determined by qPCR. **(C)** Binding of Zfx to its common target genes in ESC. ChIP using anti-epitope tag antibodies was performed on Zfx^{null} ESC reconstituted with tagged Zfx (Zfx-TAG) or on control Zfx^{null} ESC (null). The enrichment of promoter (P) or intron (I) regions of the indicated target genes in anti-tag antibody ChIP compared to control IgG ChIP was determined by qPCR. The promoter of β-actin was used as a negative control.

The regulatory regions of *Phca* could not be reliably amplified by qPCR. **(D)** A common gene induction signature of Zfx-deficient ESC and HSC. The ESC include control (Zfx^{flox}) and Zfx^{null} clones grown as undifferentiated cells or differentiated for 1 or 2 passages without LIF (Diff. P1–P2). The HSC (LSK population), myeloid progenitors and Lin^+ cells were sorted from control and Mx1-Cre^+ CKO mice 4 days after the last pI·C injection. Data represent expression levels determined by qPCR relative to the respective control SC sample (assigned an arbitrary value of 100).

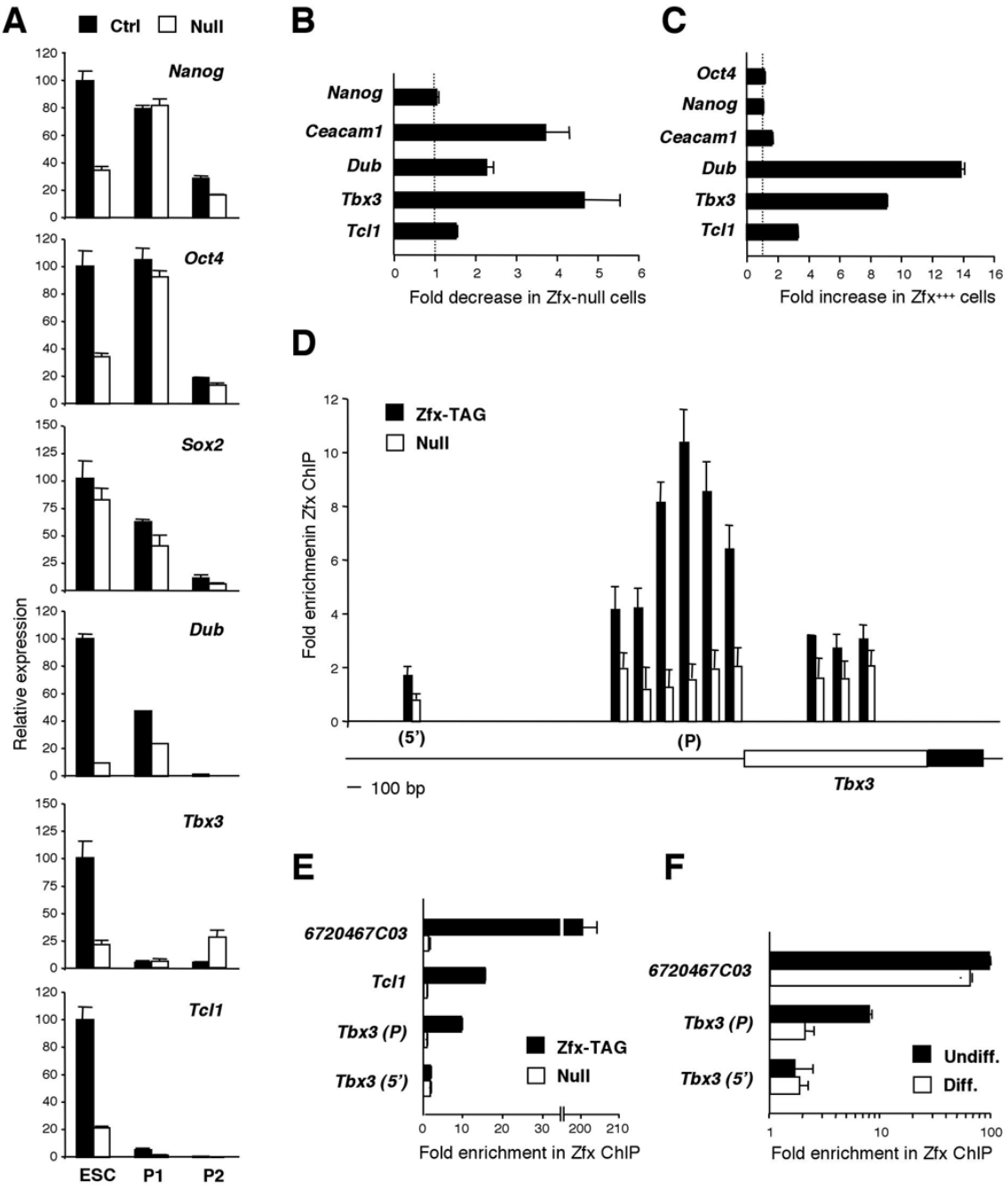

Figure 7. Zfx controls *Tbx3* and *Tcl1* expression in ESC

(A) The expression of ESC-specific genes in Zfx-deficient ESC. Control (Zfx^{flox}) and Zfx^{null} ESC clones grown in LIF or differentiated for 1 or 2 passages without LIF (P1–P2) were analyzed by qPCR. Data represent expression levels of the indicated genes relative to undifferentiated control ESC (assigned an arbitrary value of 100). **(B)** The expression of *Tbx3* and *Tcl1* in polyclonal ESC after Zfx deletion. The data represent fold decrease of the indicated genes in Zfx^{null} over control ESC in short-term batch cultures as determined by qPCR. **(C)** The expression of *Tbx3* and *Tcl1* in Zfx-overexpressing ESC as determined by qPCR. The data show fold increase of the indicated genes in Zfx-overexpressing ESC (Zfx^{null}+Zfx*, Fig. 2B) over control ESC (Zfx^{null}+Zfx). **(D)** The region of *Tbx3* promoter bound by Zfx in ESC.

The *Zfx*^{null} ESC reconstituted with tagged Zfx (Zfx-TAG) or control *Zfx*^{null} ESC were analyzed by ChIP as in Fig. 6C. Data represent the enrichment of different regions of *Tbx3* upstream region, shown below with the 5' UTR (open box) and the first coding exon (black box). **(E)** The binding of Zfx to the promoter regions of *Tbx3* and *Tcl1* in Zfx-expressing (Zfx-TAG) and Zfx-deficient (null) ESC. Shown is fold enrichment of the control target *6720467C03Rik*, *Tcl1* promoter, and *Tbx3* promoter (P) or distal 5' region (5') indicated in panel D. **(F)** Increased binding of Zfx to *Tbx3* promoter in undifferentiated versus differentiated ESC. Shown is fold enrichment of control target *6720467C03Rik*, *Tbx3* promoter (P) or distal 5' region (5') in Zfx-expressing ESC (Zfx-TAG) grown with LIF (undiff.) or differentiated for two passages without LIF (diff.).